J. Am. Chem. Soc. **1994,** *116,* 5691–5701

Oxidation of Metal-*meso*-Octaethylporphyrinogen Complexes Leading to Novel Oxidized Forms of Porphyrinogen Other than Porphyrins. 1. The Redox Chemistry of Nickel(II)- and Copper(II)-*meso*-Octaethylporphyrinogen Complexes Occurring with the Formation and Cleavage of a Cyclopropane Unit

Stefania De Angelis,[†] Euro Solari,[†] Carlo Floriani,[*,†] Angiola Chiesi-Villa,[‡] and Corrado Rizzoli[‡]

Contribution from the Institut de Chimie Minérale et Analytique, Université de Lausanne, Place du Château 3, CH-1005 Lausanne, Switzerland, and Istituto di Strutturistica Chimica, Centro di Studio per la Strutturistica Diffrattometrica del CNR, Università di Parma, I-43100 Parma, Italy

Received January 20, 1994[●]

Abstract: We report here a two-electron oxidation of a porphyrinogen tetraanion and its conversion into a dianionic form containing a cyclopropane unit [abbreviated as (Δ)]. The dianionic porphyrinogen form was structurally identified in nickel(II) and copper(II) derivatives. The redox chemistry of *meso*-octaethylporphyrinogen copper(II) helped to clarify the stepwise process leading to the oxidized form of porphyrinogen. The Ni(II)-*meso*-octaethylporphyrinogen complex [Et$_8$N$_4$NiLi$_2$(THF)$_4$] (**1**) can be converted into the oxidized form [Et$_8$N$_4$(Δ)Ni] (**3**) by reaction with excess of *p*-benzoquinone. Complex **3** contains the oxidized form of porphyrinogen which can be reduced, by lithium metal, back to complex **1**. The structural features of the oxidized form have been elucidated by X-ray crystal analysis of **2**. In contrast to the case of Ni(II), the oxidation of [Et$_8$N$_4$CuLi$_2$(THF)$_4$] (**2**) is a stepwise process initially leading to the formation of a diamagnetic square planar copper(III) derivative, [Et$_8$N$_4$Cu][Li(THF)$_4$] (**5**). Further oxidation of **5**, with CuCl$_2$, led to the monocyclopropane form of porphyrinogen in [Et$_8$N$_4$(Δ)Cu] (**4**). There is an interesting redox relationship between **2**, **4**, and **5**. The copper(III) derivative (**5**), disproportionates into **2**, containing copper(II), and **4** containing formally a copper(IV), the cyclopropane counting for a +2 oxidation state. This reaction occurs in benzene, and it can be reversed in coordinating solvents such as THF. Such a finding emphasizes the inter- and intramolecular electron-transfer processes which can occur in such systems. The best way to prepare the monocyclopropane form of porphyrinogen is, however, *via* the oxidation of **2** with *p*-benzoquinone. The X-ray analysis carried out on **2**, **4**, and **5** allows description of the major conformational changes of the porphyrinogen skeleton during the oxidation process. Crystallographic details: **2** is monoclinic, space group $C2/c$, $a = 20.808(2)$ Å, $b = 10.946(1)$ Å, $c = 22.811(2)$ Å, $\alpha = \gamma = 90°$, $\beta = 104.57(2)°$, $Z = 4$, and $R = 0.056$. **3** is orthorhombic, space group $P2_12_12_1$, $a = 11.526(1)$ Å, $b = 15.132(1)$ Å, $c = 21.098(2)$ Å, $\alpha = \beta = \gamma = 90°$, $Z = 4$, and $R = 0.057$. **4** is orthorhombic, space group $P2_12_12_1$, $a = 14.880(2)$ Å, $b = 22.050(2)$ Å, $c = 11.436(2)$ Å, $\alpha = \beta = \gamma = 90°$, $Z = 4$, and $R = 0.043$. **5** is hexagonal, space group $P3_121$, $a = b = 11.329(1)$ Å, $c = 34.939(2)$ Å, $\alpha = \beta = 90°$, $\gamma = 120°$, $Z = 3$, and $R = 0.062$.

Introduction

The oxidation of porphyrinogen is the chemical and biochemical pathway leading to the formation of the porphyrin skeleton.[1–4] Such a core originates in both cases from porphyrinogen (I, Scheme 1) *via* a six-electron oxidation requiring formally the removal of six hydrogens, four of them from the *meso*-positions (α, β, γ, and δ) (compound II).[4] The controlled oxidation of a *meso*-octaalkylporphyrinogen which does not have any *meso*-hydrogens should, in principle, shed light on the aromatization mechanism of porphyrinogen to porphyrins and/or generate other forms of oxidized porphyrinogen, a sort of "artificial porphyrin". The "acetone–pyrrole", *meso*-octamethylporphyrinogen, was discovered by A. Baeyer in 1886,[5] and since then, except for a few modifications of the synthesis,[6] it has not received much attention. A few years ago a systematic investigation of the interaction between *meso*-octaalkylporphyrinogens and transition metals was carried out in this laboratory. Studies were carried

---

[*] To whom correspondence should be addressed.

[†] Université de Lausanne.

[‡] Università di Parma.

[●] Abstract published in *Advance ACS Abstracts,* June 1, 1994.

(1) *The Porphyrins*; Dolphin, D., Ed.; Academic: New York, 1978–1979; Vols. 1–7. Smith, K. M. *Porphyrins and Metalloporphyrins*; Elsevier: Amsterdam, 1975.

(2) (a) Mashiko, T.; Dolphin, D. In *Comprehensive Coordination Chemistry*; Wilkinson, G., Gillard, R. D., McCleverty, J. A., Eds.; Pergamon: Oxford, U.K., 1987; Vol. 2, Chapter 21.1, p 855. (b) Kim, J. B.; Adler, A. D.; Longo, R. F. In *The Porphyrins*; Dolphin, D., Ed.; Academic: New York, 1978; Vol. 1, Part A, p 85. Mauzerall, D. *Ibid.* Vol. 2, p 91. (c) von Maltzan, B. *Angew. Chem., Int. Ed. Engl.* **1982,** *21,* 785. (d) Lindsey, J. S.; Schreiman, I. C.; Hsu, H. C.; Kearney, P. C.; Marguerettaz, A. M. *J. Org. Chem.* **1987,** *52,* 827. Lindsey, J. S.; Wagner, R. W. *J. Org. Chem.* **1989,** *54,* 828.

(3) (a) Angst, C.; Kajiwara, M.; Zass, E.; Eschenmoser, A. *Angew. Chem., Int. Ed. Engl.* **1980,** *19,* 140. (b) Johansen, J. E.; Piermattie, V.; Angst, C.; Diener, E.; Kratky, C.; Eschenmoser, A. *Angew. Chem., Int. Ed. Engl.* **1981,** *20,* 261. (c) Franck, B. *Angew. Chem., Int. Ed. Engl.* **1982,** *21,* 343. (d) Waditschatka, R.; Diener, E.; Eschenmoser, A. *Angew. Chem., Int. Ed. Engl.* **1983,** *22,* 631. (e) Kratky, C.; Waditschatka, R.; Angst, C.; Johansen, J. E.; Plaquevent, J. C.; Schreiber, J.; Eschenmoser, A. *Helv. Chim. Acta* **1985,** *68,* 1312. (f) Waditschatka, R.; Kratky, C.; Jaun, B.; Heinzer, J.; Eschenmoser, A. *J. Chem. Soc., Chem. Commun.* **1985,** 1604.

(4) *Biosynthesis of Tetrapyrroles*; Jordan, P. M., Ed.; Elsevier: New York, 1991.

(5) Baeyer, A. *Chem. Ber.* **1886,** *19,* 2184.

(6) (a) Fischer, H.; Orth, H. *Die Chemie des Pyrrols*; Akademische Verlagsgesellschaft: Leipzig, Germany, 1934; p 20. (b) Dennstedt, M.; Zimmermann, J. *Chem. Ber.* **1887,** *20,* 850, 2449; **1888,** *21,* 1478. (c) Dennstedt, D. *Chem. Ber.* **1890,** *23,* 1370. (d) Chelintzev, V. V.; Tronov, B. V. *J. Russ. Phys.-Chem. Soc.* **1916,** *48,* 105, 127. (e) Sabalitschka, Th.; Haase, H.; *Arch. Pharm.* **1928,** *226,* 484. (f) Rothemund, P.; Gage, C. L. *J. Am. Chem. Soc.* **1955,** *77,* 3340.

0002-7863/94/1516-5691$04.50/0

Scheme 1

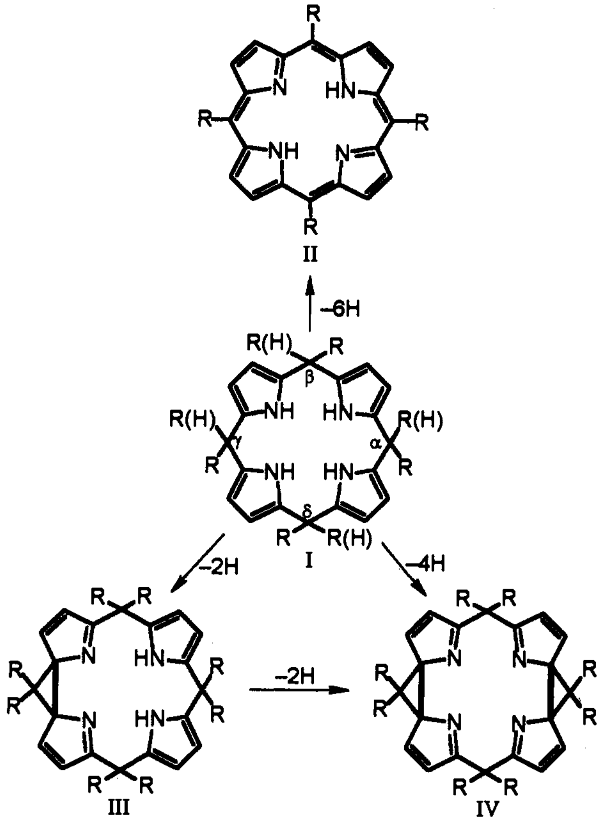

out in three major areas: (i) the metal-assisted modification of the skeleton using organometallic methodologies;[7] (ii) the organometallic functionalization of metal-porphyrinogen complexes;[8] and (iii) the redox chemistry of the metal-porphyrinogen skeleton.[9]

Here we report the generation and the chemical properties of oxidized forms by two (III) and four (IV) electrons (see Scheme 1) of *meso*-octaethylporphyrinogen tetraanion bonded to transition metals. Each cyclopropane unit forming in the absence of *meso*-hydrogens, but which can be even an intermediate in the normal aromatization of porphyrinogen,[10] functions as an electron reservoir of two electrons easily cleaved in the reduction process. The redox chemistry of such systems can be based on the formation and cleavage of cyclopropane units.

Important inter- and intramolecular electron transfer between the metal and the cyclopropane unit has been synthetically detected. The first paper of this series deals with the generation, the chemistry, and the metal-ligand redox relationship of the monocyclopropane form III with *meso*-octaethylporphyrinogen by investigation of the redox chemistry of *meso*-octaethylporphyrinogen-nickel(II) and -copper(II) complexes. Preliminary results in this area have been briefly communicated in the case of cobalt.[9b] In the second paper of this series we will report the introduction of a second cyclopropane unit in the oxidized form IV of the porphyrinogen.

Results and Discussion

The starting materials we have considered for studying the synthetic consequences of oxidation on the *meso*-octaalkylporphyrinogen skeleton are compounds derived from the complexation of $NiCl_2$ and $CuCl_2$ with the lithiated form, $[Et_8N_4Li_4(THF)_4]$,[8a] of *meso*-octaethylporphyrinogen, $Et_8N_4H_4$.

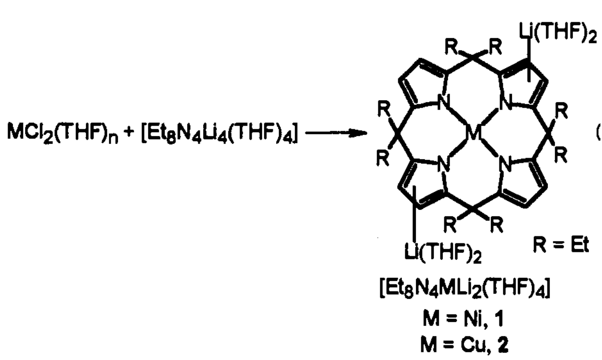

(1)

The synthesis and the structure of **2**, and its isostructural Fe(II) and Co(II) derivatives, have recently been described by this group;[7b] **1** is reported here. The solid-state structure of **2** is described along the other copper complexes (*vide infra*). Complex **1**, which is isostructural with **2**,[11] is a diamagnetic compound which has been fully characterized. The ^1H NMR spectrum shows a singlet for all 3,4 protons of the pyrrolyl anions, while the ethyl groups appear as two sets of peaks. Nonequivalent ethyl groups are a general phenomenon and can be explained from the structure in the solid state. Two ethyl groups above and below are bent toward the metal center, while the other two pairs point out of the porphyrinogen core.[9a,7b] The equivalence of all of the four pyrrolyl rings as well as the top and the bottom faces of the ligand can be accounted for by assuming that lithium cations rapidly exchange intra- and intermolecularly among the eight possible positions. Complexes **1** and **2**, which contain, in addition to the transition metal bonded for the four nitrogens, the lithium cation η^3-bonded to two pyrrolyl anions,[7b] are very sensitive to several oxidizing agents. This sensitivity to oxidation is also shared by the lithium derivative $[Et_8N_4Li_4(THF)_4]$ and to a lesser extent by $Et_8N_4H_4$. The use of a specific oxidizing agent is particularly crucial for the isolation and the yield of the oxidized forms of III and IV (Scheme 1). In a preliminary stage we measured the absorption of molecular oxygen. In all experiments, regardless of the metal (Ni, Cu, or Li), 4 mol of O_2 were absorbed *per* porphyrinogen unit. Although there is consistency in this rather intriguing and unaccountable stoichiometry, the isolation of products was, except in a few cases, unsuccessful.[9b] Thus we turned to use of quinones, which have been employed in the dehydrogenation of different porphyrinogens, though the reaction should not in this case involve any dehydrogenation.[10] The success of the reaction is essentially based on the appropriate redox potential of the *p*-benzoquinone used and on its conversion into a compound which has a solubility different than that of the oxidized form of porphyrinogen.

Ethereal solutions of **1** and **2** were reacted with a diethyl ether solution of *p*-benzoquinone. A rapid reaction occurs with the precipitation of a mixture of a blue and a red solid and formation of a red solution in both cases. A quantitative recovery of **3** and **4** was carried out by extracting the solid mixture using the mother liquor (see the Experimental Section).

In such a way the red crystalline solids **3** and **4** have been easily separated from the rather insoluble blue solid, which we believe to be the lithiated form of quinhydrone. The reaction requires at least a 2:1 quinone:metal ratio, the actual ratio we used being 4:1 for nickel and 2:1 for copper. The yields of **3** and **4** are reasonably high, and the reaction can be carried out on a multigram scale.

---

[7] (a) Jacoby, D.; Floriani, C.; Chiesi-Villa, A.; Rizzoli, C. *J. Am. Chem. Soc.* **1993**, *115*, 7025. (b) Jubb, J.; Jacoby, D.; Floriani, C.; Chiesi-Villa, A.; Rizzoli, C. *Inorg. Chem.* **1992**, *31*, 1306.

[8] (a) Jacoby, D.; Floriani, C.; Chiesi-Villa, A.; Rizzoli, C. *J. Am. Chem. Soc.* **1993**, *115*, 3595. (b) Jacoby, D.; Floriani, C.; Chiesi-Villa, A.; Rizzoli, C. *J. Chem. Soc., Chem. Commun.* **1991**, 790.

[9] (a) Jacoby, D.; Floriani, C.; Chiesi-Villa, A.; Rizzoli, C. *J. Chem. Soc., Chem. Commun.* **1991**, 220. (b) Jubb, J.; Floriani, C.; Chiesi-Villa, A.; Rizzoli, C. *J. Am. Chem. Soc.* **1992**, *114*, 6571.

[10] Reference 4, Chapters 2.3 and 2.4.

[11] Crystal data for $C_{52}H_{80}Li_2N_4NiO_4$: monoclinic, space group $C2/c$, $a = 20.588(2)$ Å, $b = 10.975(1)$ Å, $c = 22.748(2)$ Å, $\beta = 105.27(2)°$, $V = 4958.5(9)$ Å^3, $MW = 897.8$, $Z = 4$, $d_{calcd} = 1.203$ g cm^{-3}, $\mu(Cu\ K\alpha) = 8.90$ cm^{-1}, $\lambda = 1.54178$ Å. The X-ray analysis has not been carried out.

Table 1. Experimental Data for the X-ray Diffraction Studies on Crystalline Compounds **2**, **3**, **4**, and **5**

	2	**3**	**4**	**5**
chemical formula	$C_{52}H_{80}CuLi_2N_4O_4$	$C_{36}H_{48}N_4Ni{\cdot}C_4H_8O$	$C_{36}H_{48}CuN_4{\cdot}C_6D_6$	$C_{36}H_{48}CuN_4{\cdot}C_{16}H_{32}LiO_4$
a (Å)	20.808(2)	11.526(1)	14.880(2)	11.329(1)
b (Å)	10.946(1)	15.132(1)	22.050(2)	11.329(1)
c (Å)	22.811(2)	21.098(2)	11.436(2)	34.939(2)
α (deg)	90	90	90	90
β (deg)	104.57(2)	90	90	90
γ (deg)	90	90	90	120
V (Å^3)	5028.5(9)	3679.7(5)	3752.2(9)	3883.5(5)
Z	4	4	4	3
fw	902.7	667.6	676.3	895.7
space group	$C2/c$ (no. 15)	$P2_12_12_1$ (no. 19)	$P2_12_12_1$ (no. 19)	$P3_121$ (no. 152)
t (°C)	22	22	22	22
λ (Å)	1.541 78	1.541 78	1.541 78	1.541 78
ρ_{calcd} (g cm^{-3})	1.192	1.205	1.197	1.149
μ (cm^{-1})	9.32	9.91	10.31	9.04
transmn coeff	0.782–1.000	0.835–1.000	0.899–1.000	0.874–1.000
R^a	0.056	0.057 [0.060]^c	0.043 [0.046]^c	0.062
R^b	0.059	0.063 [0.066]		

^{a} $R = \sum|\Delta F|/\sum|F_o|$. ^{b} $R_w = \sum w^{1/2}|\Delta F|/\sum w^{1/2}|F_o|$. ^{c} The values in square brackets refer to the inverted structure.

Table 2. Fractional Atomic Coordinates (×10^4) for Complex **2**

atom	x/a	y/b	z/c
Cu1	0(–)	2274.6(7)	2500(–)
Li1	1478(4)	3439(8)	1572(4)
O1	2250(2)	3853(4)	1257(2)
O2	874(2)	4661(3)	1159(2)
N1	852(1)	2254(3)	2285(1)
N2	465(1)	2192(3)	3345(1)
C1	974(2)	1570(3)	1818(2)
C2	1655(2)	1492(4)	1887(2)
C3	1960(2)	2164(4)	2419(2)
C4	1453(2)	2609(3)	2658(2)
C5	1478(2)	3312(4)	3237(2)
C6	1090(2)	2602(4)	3612(2)
C7	1258(2)	2287(4)	4223(2)
C8	705(2)	1646(4)	4330(2)
C9	227(2)	1605(3)	3791(2)
C10	–420(2)	884(4)	3620(2)
C11	1138(2)	4580(4)	3075(2)
C12	1479(2)	5449(4)	2719(2)
C13	2214(2)	3475(5)	3596(2)
C14	2351(2)	4358(6)	4125(2)
C15	–268(2)	–302(4)	3310(2)
C16	–843(3)	–1098(5)	3014(3)
C17	–632(2)	529(4)	4199(2)
C18	–810(2)	1553(5)	4573(2)
C21	2401(4)	3566(11)	710(4)
C22	3045(6)	3852(13)	743(5)
C23	3358(4)	4222(10)	1335(5)
C24	2831(4)	4330(8)	1621(3)
C25	201(3)	4758(5)	1184(3)
C26	–42(4)	5937(7)	925(4)
C27	474(4)	6505(7)	709(4)
C28	1046(4)	5767(8)	903(4)

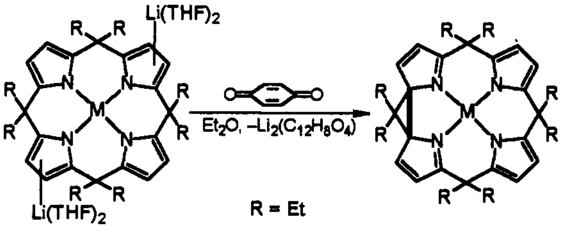

(2)

[Et$_8$N$_4$MLi$_2$(THF)$_4$]
1, M = Ni
2, M = Cu

[Et$_8$N$_4$(Δ)M]
3, M = Ni
4, M = Cu

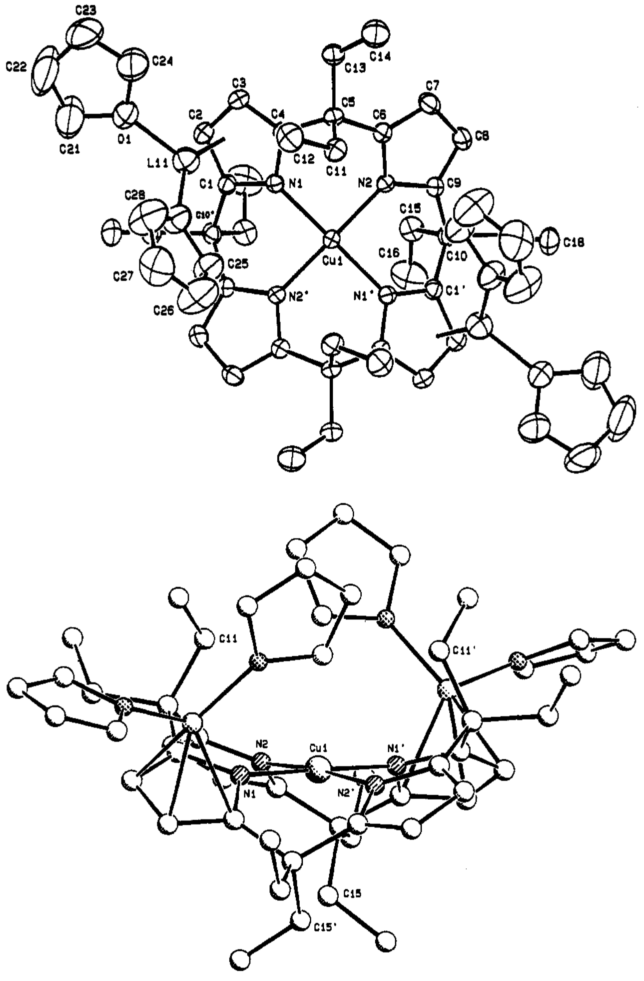

Figure 1. (top) ORTEP view of complex **2** (30% probability ellipsoids). Primes denote a transformation of $-x, y, 0.5 - z$. (bottom) A perspective view (SCHAKAL) of complex **2**.

An alternative oxidation of **1** was carried out using I_2. The yield is, however, significantly lower, and the product cannot be extracted from significant amounts of LiI (see the Experimental Section). Reaction 2 corresponds to a two-electron oxidation leading to the introduction of a cyclopropane unit into the porphyrinogen skeleton. Formation of C—C bonds by a reductive coupling of the C═X functionality is a classic organometallic reaction,[12] while the oxidative coupling is much less known, at least as an intramolecular process. In addition, such C—C bonds when formed are hard to oxidize. In previous work we discovered a C—C bond functioning as a two-electron shuttle.[13] The bond

---

[12] Collman, J. P.; Hegedus, L. S.; Norton, J. R.; Finke, R. G. *Principles and Applications of Organotransition Metal Chemistry*; University Science Books: Mill Valley, CA, 1987.

Table 3. Fractional Atomic Coordinates ($\times 10^4$) for Complex **3**[a]

atom	*x/a*	*y/b*	*z/c*	atom	*x/a*	*y/b*	*z/c*
Ni1	3642.0(7)	–2510.7(5)	1667.8(4)	C22	26(7)	–2995(6)	2267(4)
N1	3166(4)	–2957(3)	2441(2)	C23	1065(6)	–4865(4)	2159(4)
N2	3334(4)	–3549(3)	1231(2)	C24A	1757(9)	–5653(7)	2350(5)
N3	4266(4)	–2006(3)	934(2)	C24B	265(24)	–5147(18)	1767(13)
N4	4079(4)	–1449(3)	2044(2)	C25	6038(6)	–3729(4)	552(3)
C1	3555(5)	–2693(3)	3041(3)	C26	6337(7)	–3594(5)	1249(4)
C2	3071(6)	–3237(4)	3486(3)	C27	4742(5)	–3456(4)	–378(3)
C3	2359(6)	–3850(4)	3165(3)	C28	3672(6)	–3056(6)	–677(3)
C4	2428(5)	–3672(4)	2520(3)	C29	3776(6)	512(4)	872(3)
C5	1735(5)	–4014(4)	1975(3)	C30	3420(7)	588(5)	181(4)
C6	2534(5)	–4174(4)	1408(3)	C31	2338(5)	–737(4)	1152(3)
C7	2560(6)	–4849(4)	977(3)	C32	1650(7)	–282(5)	1704(4)
C8	3388(7)	–4629(4)	506(3)	C33	3801(7)	–1348(4)	3712(3)
C9	3857(5)	–3823(4)	676(3)	C34	2614(8)	–968(5)	3522(3)
C10	4852(5)	–3340(4)	348(3)	C35	5558(7)	–2205(4)	3397(3)
C11	4872(5)	–2383(4)	483(2)	C36	6237(6)	–2694(5)	2881(4)
C12	5603(6)	–1730(4)	177(3)	C41	257(13)	2673(11)	1(7)
C13	5465(6)	–953(4)	470(3)	C42A	–442(16)	2002(13)	266(9)
C14	4560(5)	–1083(4)	947(2)	C43A	225(28)	1920(19)	946(12)
C15	3599(5)	–436(3)	1129(2)	C44A	1187(21)	2623(17)	940(11)
C16	4443(5)	–728(3)	1642(3)	C45A	747(26)	3173(15)	515(12)
C17	5175(5)	–156(4)	2036(3)	C42B	–497(24)	2424(22)	606(15)
C18	5188(6)	–479(4)	2609(3)	C43B	204(19)	1463(13)	602(10)
C19	4490(5)	–1295(3)	2612(3)	C44B	1370(21)	1815(16)	796(11)
C20	4328(6)	–1901(4)	3170(3)	C45B	1500(22)	2709(18)	444(13)
C21	826(5)	–3314(4)	1755(3)				

[a] The site occupation factors are 0.5 for C42, C43, C44, and C45 (A and B) and 0.75 and 0.25 for C24A and C24B, respectively.

Table 4. Fractional Atomic Coordinates ($\times 10^4$) for Complex **4**

atom	*x/a*	*y/b*	*z/c*	atom	*x/a*	*y/b*	*z/c*
Cu1	2391.9(5)	3458.4(4)	6602.4(8)	C20	1674(4)	2029(3)	5935(6)
N1	2797(3)	2684(2)	7098(4)	C21	3335(5)	3314(3)	9407(6)
N2	3510(3)	3855(2)	6856(4)	C22	3025(6)	2822(4)	10229(8)
N3	1886(3)	4206(2)	5908(5)	C23	4885(5)	2920(3)	9002(6)
N4	1232(3)	3118(2)	6119(4)	C24	5633(4)	2696(3)	8187(7)
C1	2497(4)	2129(2)	6691(6)	C25	3685(5)	4437(4)	4127(7)
C2	3061(4)	1689(3)	7100(6)	C26	3522(6)	3778(4)	3906(7)
C3	3740(4)	1976(3)	7776(6)	C27	3497(5)	5382(3)	5326(7)
C4	3569(4)	2589(3)	7747(5)	C28	3120(7)	5703(4)	6358(8)
C5	3991(4)	3116(2)	8417(6)	C29	–691(4)	4313(3)	6061(7)
C6	4154(4)	3665(3)	7632(6)	C30	–727(5)	4989(4)	6292(8)
C7	4841(4)	4079(4)	7615(8)	C31	440(4)	4030(3)	7704(6)
C8	4622(5)	4529(3)	6794(7)	C32	–131(5)	3566(4)	8355(8)
C9	3790(4)	4385(3)	6343(6)	C33	1033(4)	1568(3)	6556(7)
C10	3315(5)	4689(3)	5308(6)	C34	659(5)	1771(4)	7727(8)
C11	2314(4)	4586(3)	5262(5)	C35	1971(5)	1757(3)	4750(7)
C12	1709(5)	4863(3)	4394(6)	C36	2553(5)	2183(4)	4032(6)
C13	903(5)	4594(3)	4528(6)	C41	7763(4)	6040(2)	4067(5)
C14	964(5)	4183(3)	5532(6)	C42	7270(4)	6057(2)	5104(5)
C15	225(4)	4045(3)	6384(6)	C43	6767(4)	5553(2)	5447(5)
C16	563(4)	3523(3)	5645(5)	C44	6758(4)	5033(2)	4754(5)
C17	33(5)	3155(4)	4826(6)	C45	7251(4)	5016(2)	3717(5)
C18	334(4)	2586(3)	4875(7)	C46	7754(4)	5519(2)	3374(5)
C19	1102(4)	2585(3)	5671(6)				

forms intermolecularly from a reductive coupling of the imino groups across two tetradentate Schiff base complexes, and it is easily cleaved by oxidants under mild conditions. The structural characterization of **3** can be carried out both in the solid state and by solution NMR, as it is diamagnetic. The cyclopropane unit introduces a significant deviation in the pyrrolyl protons, and this part of the NMR spectrum can be considered diagnostic for the presence of a cyclopropane unit (see the Experimental Section). The solid-state structure of **3** is shown in Figure 2 (top and bottom), while the structure of **4** will be discussed jointly with the related copper complexes (*vide infra*).

In Tables 6 and 7 selected bond distances and angles for complexes **2**, **3**, **4**, and **5** are listed. In Table 8 the most relevant conformational parameters for complexes **2**, **3**, **4**, and **5** are quoted. The pyrrole rings containing N1, N2, N3, and N4 are labeled A, B, C, and D, respectively.

Complex **3** (Figure 2 (top and bottom)) crystallizes with disordered THF solvent molecules in a 1:1 molar ratio. The Ni–N bond distances fall in a rather narrow range [1.849(4)–1.870(4) Å]. The N_4 core is planar, the nickel atom deviating by 0.060(1) Å from that plane (Table 8). Bond distances and angles within the ligand are consistent with a double bond localization on the N3–C11, N4–C19, C12–C13, and C17–C18 bonds of the C and D pyrrole rings as a consequence of the cyclopropane formation. Accordingly the N3–C14 and N4–C16 distances and the C–C distances adjacent to the macro-ring (C11–C12, C13–C14, C16–C17, and C18–C19) have single bond character (Table 6). A significant amount of delocalization is observed for pyrroles A and B, while C and D have localized double bonds.

The oxidized form of *meso*-octaethylporphyrinogen (form III, Scheme 1) assumes a conformation with the pyrrole rings tilted on the same side with respect to the N_4 core. The significant differences observed in the dihedral angles between the N_4 plane

---

[13] Gallo, E.; Solari, E.; De Angelis, S.; Floriani, C.; Re, N.; Chiesi-Villa, A.; Rizzoli, C. *J. Am. Chem. Soc.* **1993**, *115*, 9850 and references therein.

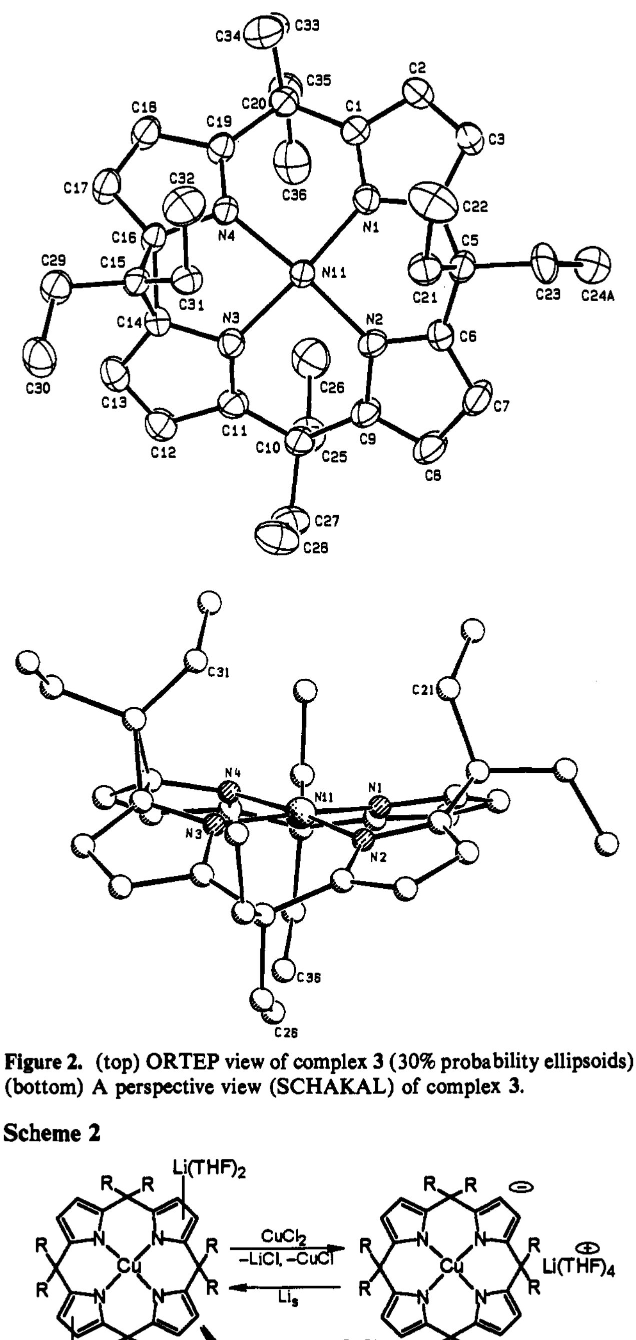

Figure 2. (top) ORTEP view of complex **3** (30% probability ellipsoids). (bottom) A perspective view (SCHAKAL) of complex **3**.

Scheme 2

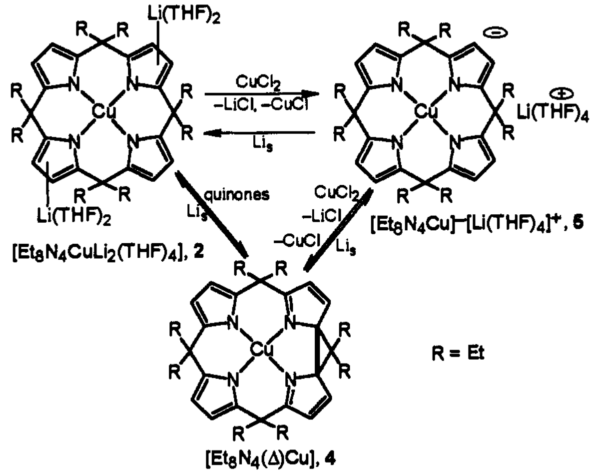

Scheme 3

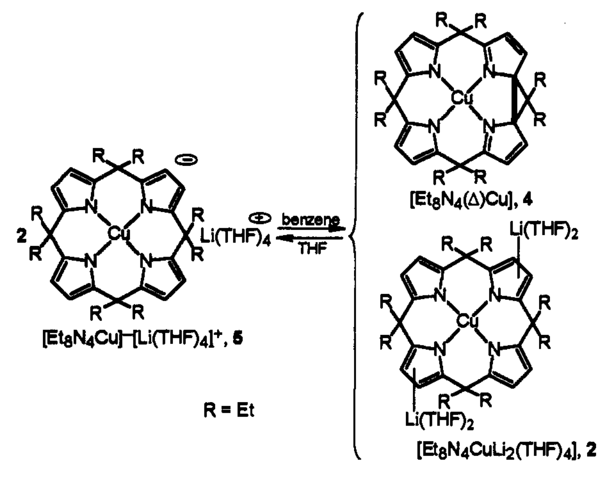

and the pyrrole rings (Table 8) are small and can be related to the asymmetry of the molecule introduced by the cyclopropane. The most significant difference within the structural parameters concerns the nickel out-of-plane distances from the pyrrole rings, the largest deviations being observed for the C and D rings (Table 8). The conformation of the ligand leads to two methylenic groups (C21 and C31) above and two methyl groups (C26 and C36) below the coordination plane. Only one hydrogen (H311 from the C31 methylenic group) approaches the metal at a distance of 2.69 Å, the other Ni···H contacts being greater than 3.0 Å. This is consistent with the closest approach of C31 to the metal (Ni···C31, 3.263(6) Å; Ni···C21, 3.471(6) Å; Ni···C26, 3.622(6) Å; Ni···C36, 3.946(6) Å). Such short distances can be viewed as a three-center four-electron interaction,[14] though we cannot prove this by IR and NMR spectroscopies, or they too may arise simply from rigid or sterically constrained ligands.[15] The configurations of the two asymmetric carbon atoms are *S* for C14 and *R* for C16 (*vide infra*).

The oxidized form of porphyrinogen containing a cyclopropane unit has only minor differences from the reduced form **1**, the structural parameters of which can be determined from the isostructural Fe, Co, Ni, and Cu complexes. The C–C bond formation, closing up the saddle shape conformation, only slightly changes the nearly square planar coordination of the metal, but an interaction is observed between the metal and the peripheric ethyl groups and the C···C distance moves from an average value of *ca.* 2.50 Å, in the reduced form, to a bonding interaction at 1.567(8) Å for C14–C16 in **3**. The relatively small molecular reorganization required by the cyclopropane formation may imply that the process can be easily reversed.

The reaction of **3** with lithium metal in the presence of biphenyl led almost quantitatively to **1**. The use of metal Li in a heterogeneous phase in the absence of biphenyl was unsuccessful.

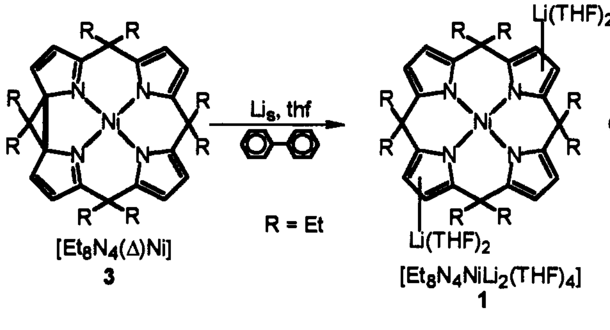

(3)

The formation and cleavage of a cyclopropane unit within the porphyrinogen skeleton is clearly a two-electron redox process. This implies that under appropriate conditions the cyclopropane unit functions as an electron reservoir for two electrons. The questions which arise at this point are the following: (i) Does the metal assist in the redox process? (ii) Can two monoelectronic

---

[14] Anklin, C. G.; Pregosin, P. S. *Magn. Reson. Chem.* **1985**, *23*, 671. Brammer, L.; Charnock, J. M.; Goggin, P. L.; Goodfellow, R. J.; Orpen, A. G.; Koetzle, T. F.; *J. Chem. Soc., Dalton Trans.* **1991**, 1789. Wehman-Ooyevaar, I. C. M.; Grove, D. M.; Kooijman, H.; van der Sluis, P.; Speck, A. L.; van Koten, G. *J. Am. Chem. Soc.* **1992**, *114*, 9916.

[15] Sunquist, W. I.; Bancroft, D. P.; Lippard, S. J. *J. Am. Chem. Soc.* **1990**, *112*, 1590.

Table 5. Fractional Atomic Coordinates (×10^4) for Complex **5**[a]

atom	*x/a*	*y/b*	*z/c*	atom	*x/a*	*y/b*	*z/c*
Cu1	–119.3(12)	–119.3(12)	0(–)	C15	1451(12)	3198(8)	–350(3)
Li1	0(–)	4734(23)	1667(–)	C16	1835(14)	4423(11)	–110(3)
O1	1223(10)	4349(9)	1384(3)	C17	–404(12)	3291(9)	–743(3)
O2	–1075(12)	5128(10)	1319(3)	C18A	–1720(21)	2672(21)	–868(6)
N1	33(5)	–301(5)	526(1)	C18B	548(21)	4034(21)	–1052(6)
N2	–1052(6)	828(6)	87(2)	C21A	711(26)	2915(27)	1255(7)
C1	1158(8)	–225(9)	708(2)	C21B	849(34)	3800(38)	971(11)
C2	915(10)	–294(11)	1095(2)	C22	1716(25)	3248(19)	930(6)
C3	–354(9)	–376(10)	1146(2)	C23A	3036(31)	4095(35)	1201(9)
C4	–890(7)	–374(9)	793(2)	C23B	2746(30)	4466(31)	895(8)
C5	–2232(8)	–506(9)	665(2)	C24A	2629(33)	4819(31)	1454(9)
C6	–1872(8)	628(8)	391(2)	C24B	2570(48)	5164(36)	1213(12)
C7	–2313(10)	1568(11)	354(3)	C25A	–1983(42)	5631(37)	1428(9)
C8	–1749(12)	2326(11)	26(3)	C25B	–974(39)	6295(40)	1252(12)
C9	–968(8)	1853(8)	–134(2)	C26A	–2982(43)	5039(46)	1093(15)
C10	–29(10)	2363(8)	–480(3)	C26B	–1255(39)	6072(36)	837(12)
C11	–2985(10)	–334(9)	1018(2)	C27	–2307(30)	4980(26)	777(6)
C12	–3634(14)	–1526(10)	1296(3)	C28A	–839(31)	5250(32)	877(10)
C13	–3094(8)	–1910(8)	469(2)	C28B	–2501(35)	4151(35)	1159(11)
C14	–4450(11)	–2119(8)	300(3)				

[a] The site occupation factors are 0.5 for C21, C23, C24, C25, C26, and C28 (A and B) and 0.6 and 0.4 for C18 (A and B, respectively).

Table 6. Selected Bond Distances (Å) and Angles (deg) for Complexes **3** and **4** (M = Ni and Cu for **3** and **4**, Respectively)

	3	**4**		**3**	**4**
M–N1	1.849(4)	1.897(5)	C5–C6	1.529(9)	1.526(9)
M–N2	1.856(5)	1.902(5)	C6–C7	1.368(9)	1.371(10)
M–N3	1.870(4)	1.979(5)	C7–C8	1.417(10)	1.404(12)
M–N4	1.861(5)	1.962(5)	C8–C9	1.381(9)	1.378(10)
N1–C1	1.401(8)	1.383(7)	C9–C10	1.526(8)	1.533(10)
N1–C4	1.386(8)	1.384(7)	C10–C11	1.476(9)	1.508(10)
N2–C6	1.373(8)	1.372(8)	C11–C12	1.450(9)	1.473(9)
N2–C9	1.381(8)	1.372(8)	C12–C13	1.338(9)	1.347(10)
N3–C11	1.311(7)	1.286(8)	C13–C14	1.463(8)	1.466(10)
N3–C14	1.438(8)	1.439(9)	C14–C15	1.527(8)	1.500(10)
N4–C16	1.444(7)	1.443(8)	C14–C16	1.567(8)	1.578(9)
N4–C19	1.309(8)	1.297(8)	C15–C16	1.521(8)	1.514(9)
C1–C2	1.368(9)	1.365(8)	C16–C17	1.467(8)	1.469(10)
C1–C20	1.518(8)	1.515(9)	C17–C18	1.304(9)	1.333(11)
C2–C3	1.412(9)	1.421(9)	C18–C19	1.474(8)	1.461(9)
C3–C4	1.389(9)	1.376(9)	C19–C20	1.504(9)	1.523(9)
C4–C5	1.493(9)	1.527(8)			
N3–M–N4	84.1(2)	82.6(2)	M–N4–C19	129.9(4)	126.1(4)
N2–M–N4	173.9(2)	171.4(2)	M–N4–C16	118.7(4)	118.4(4)
N2–M–N3	90.5(2)	90.6(2)	C16–N4–C19	107.3(4)	108.0(5)
N1–M–N4	91.1(2)	91.1(2)	N1–C1–C20	125.1(5)	125.6(4)
N1–M–N3	173.6(2)	172.1(2)	N1–C1–C2	108.5(5)	108.4(5)
N1–M–N2	94.1(2)	95.2(2)	C2–C1–C20	126.3(6)	126.1(5)
M–N1–C4	125.0(4)	124.1(4)	N1–C4–C3	107.7(5)	108.4(5)
M–N1–C1	126.7(4)	126.4(4)	C3–C4–C5	131.0(6)	131.3(6)
C1–N1–C4	108.1(4)	108.3(5)	N1–C4–C5	120.4(5)	119.7(5)
M–N2–C9	126.3(4)	126.3(4)	C4–C5–C6	109.6(5)	111.9(5)
M–N2–C6	125.2(4)	124.7(4)	N2–C6–C5	120.5(5)	120.8(5)
C6–N2–C9	108.5(5)	108.9(5)	C5–C6–C7	130.7(5)	130.9(6)
M–N3–C14	118.1(3)	117.0(4)	N2–C6–C7	108.6(5)	108.0(6)
M–N3–C11	128.9(4)	125.8(4)	N2–C9–C8	108.3(5)	108.0(6)
C11–C3–C14	108.1(4)	108.9(5)	C8–C9–C10	126.8(6)	127.0(6)
N2–C9–C10	124.7(5)	124.2(5)	C14–C15–C16	61.9(3)	63.1(4)
C9–C10–C11	113.2(5)	114.6(5)	C14–C16–C15	59.3(3)	58.0(4)
N3–C11–C10	124.0(5)	124.6(6)	N4–C16–C15	116.8(4)	119.3(5)
C10–C11–C12	126.3(5)	124.4(5)	N4–C16–C14	108.4(4)	109.9(5)
N3–C11–C12	109.6(5)	110.8(5)	C15–C16–C17	126.8(4)	126.7(6)
N3–C14–C13	106.6(5)	105.7(6)	C14–C16–C17	133.1(5)	131.3(6)
C13–C14–C16	131.2(5)	127.7(6)	N4–C16–C17	106.3(5)	105.5(5)
C13–C14–C15	127.1(4)	126.1(6)	N4–C19–C18	110.0(5)	111.2(6)
N3–C14–C16	109.3(4)	111.6(5)	C18–C19–C20	125.6(5)	124.2(6)
N3–C14–C15	117.2(5)	120.8(6)	N4–C19–C20	124.3(5)	124.6(6)
C15–C14–C16	58.8(3)	58.8(4)	C1–C20–C19	114.4(5)	116.6(5)

steps be eventually identified with the isolation of the corresponding species?

In the case of nickel, due to its great stability in the oxidation state (+2), the assistance of the metal may be difficult to single out. A clear answer to both questions comes from examining the reaction of **2** with $CuCl_2$, which is used as a selective unielectronic oxidizing agent. The results have been summarized in Scheme 2.

When 1 mol of solid $CuCl_2$ is added to a red solution of **2** in THF, a blue solution is rapidly formed, and a blue solid can be isolated (85%) in crystalline form (step a). The blue complex **5** contains a Cu(III) ion, and its diamagnetism allows an NMR characterization. The ^{1}H NMR spectrum is very similar to that of the isoelectronic Ni(II) complex, **1**, with a singlet for the pyrrolyl protons and two sets of different ethyl groups. Further oxidation of the blue THF solution of **5**, with 1 mol of $CuCl_2$, led to a red-violet solution of **4**, which was isolated (81%) as a crystalline solid (step *b*). In the case of copper the cyclopropane formation is a clear two-step monoelectronic oxidation. The second step of Scheme 2 corresponds to a reduction of Cu(III) to Cu(II) with the concomitant formation of the cyclopropane unit. This result emphasizes the intramolecular redox relationship between the metal and the ligand. The copper(II)–cyclopropane fragment can be considered as the highest oxidation state of the systems we have so far inspected. The redox process can be reversed using a stoichiometric amount of lithium metal to reduce **4** to **5**, and then **5** to **2** (see the Experimental Section).

It is worth emphasizing the importance of the +III oxidation state of copper,[16,17] obtained by using a tetrapyrrolic structure, and its relationship with copper(II) mediated by the ligand. We found that its stability is, however, associated to the solvents that come in contact with it. When a benzene solution of **5** was kept for 2 days at 5–10 °C, a crystalline red-violet and a crystalline orange solid separate. Crystals selected were found to be an equimolar mixture of **2** and **4**. In this case complex **4** crystallizes with a molecule of benzene. Crystals were selected for the X-ray analysis and found to be a better quality than those obtained from reaction 2. In support of the solvent-dependent disproportionation reaction shown in Scheme 3, we found that an equimolar solution of **2** and **4** in THF rapidly forms a blue solution from which **5** can be quantitatively crystallized (93%).

The sequence of reactions shown in Scheme 2 clearly indicates the presence of an intramolecular redox process between Cu(II), Cu(III), and the cyclopropane unit, while in the disproportionation of **5** and in the reverse reaction (Scheme 3), we are dealing with an intermolecular electron transfer. The association between metal–porphyrinogens allowing intermolecular electron transfers may be, in this context, a very crucial factor. This association can be assisted by the lithium cation depending on the competitive binding with either the periphery of the porphyrinogen or the solvent. There are a significant number of structurally identified examples where an alkali cation is bridging two porphyrinogen units using the electron-rich pyrrolyl anion.[7a,8a] This idea is further supported by the behavior of **6** obtained by replacing the THF molecules around the Li cation in **5** by 12-crown-4 (reaction 4).

$$\underset{\mathbf{5}}{[Et_8N_4Cu]^-Li(THF)_4^+} + \text{12-crown-4} \rightarrow \underset{\mathbf{6}}{[Et_8N_4Cu]^-[Li(12\text{-crown-4})]^+} \quad (4)$$

Complex **6** does not disproportionate in the presence of either benzene or CH_2Cl_2. Clearly a solvation effect is controlling the electron-transfer process outlined in Scheme 3. The relationship outlined above between **2**, **4**, and **5** suggests that the molecular rearrangement converting one species to another is facile. In this context, it is helpful to consider the structural relationship between **2**, **4**, and **5**.

Table 7. Selected Bond Distances (Å) and Angles (deg) for Complexes **2** and **5**[a]

	2	**5**
Cu1–N1	1.955(2)	1.867(4)
Cu1–N2	1.929(2)	1.869(9)
N1–C1	1.377(5)	1.388(11)
N1–C4	1.380(4)	1.373(10)
N2–C6	1.366(4)	1.353(11)
N2–C9	1.395(5)	1.358(12)
C1–C2	1.388(6)	1.374(10)
C1–C10′	1.520(5)	1.498(14)
C2–C3	1.424(6)	1.405(17)
C3–C4	1.392(7)	1.375(11)
C4–C5	1.518(6)	1.519(13)
C5–C6	1.528(7)	1.486(12)
C6–C7	1.392(6)	1.390(18)
C7–C8	1.420(6)	1.382(14)
C8–C9	1.374(6)	1.363(18)
C9–C10	1.524(6)	1.521(13)
N2–Cu1–N2′	174.6(1)	179.5(3)
N1–Cu1–N2′	90.4(1)	89.2(3)
N1–Cu1–N2	89.5(1)	90.7(3)
N1–Cu1–N1′	178.7(1)	179.0(2)
Cu1–N1–C4	125.5(2)	124.5(5)
Cu1–N1–C1	123.8(2)	125.2(4)
C1–N1–C4	108.4(3)	109.9(5)
Cu1–N2–C9	124.7(2)	125.5(6)
Cu1–N2–C6	127.7(2)	124.7(5)
C6–N2–C9	107.4(3)	109.8(7)
N1–C1–C2	109.1(3)	107.2(8)
N1–C1–C10′	121.3(3)	120.4(7)
C2–C1–C10′	128.9(4)	132.3(8)
N1–C4–C3	108.6(3)	106.6(8)
C3–C4–C5	130.9(4)	133.2(7)
N1–C4–C5	120.4(4)	120.0(6)
C4–C5–C6	108.8(3)	106.0(8)
N2–C6–C5	119.7(4)	121.3(8)
C5–C6–C7	130.6(4)	132.3(8)
N2–C6–C7	109.6(4)	106.2(7)
N2–C9–C8	109.1(3)	108.7(8)
C8–C9–C10	129.8(4)	130.2(8)
N2–C9–C10	120.3(3)	120.9(8)
C1′–C10–C9	112.8(3)	108.6(7)

[a] ′ = $-x, y, {}^1/_2 - z$ for **2**. ′ = $y, x, -z$ for **5**.

An ORTEP drawing and a perspective view of complex **2** are shown in Figure 1, top and bottom, respectively. In compounds **2** and **5** the complex molecules possess crystallographically imposed C_2 symmetries with the 2-fold axis running through copper and perpendicular to the N_4 core. In **2**, two symmetry-related $[Li(THF)_2]^+$ cations are anchored to opposite A and C pyrrole rings (see the previous labeling concerning the pyrrole rings adopted for **3**). The range of the Li–N [2.663(10) Å] and Li–C distances [Li1–C1, 2.428(10) Å; Li1–C2, 2.250(10) Å; Li1–C3, 2.390(9) Å; Li1–C4, 2.651(10) Å] suggests a preferential Li^+–pyrrole η^3-interaction rather than an η^5-interaction. The geometry of the $[Et_8N_4Cu]^{2-}$ skeleton in **2** is comparable with that of the $[Et_8N_4Cu]^-$ anion in **5**, where the counterion is $[Li(THF)_4]^+$, and cations are separated from the anions by van der Waals interactions. An ORTEP drawing and a perspective view of complex **5** are given in Figure 4, top and bottom, respectively. The most significant difference between the two complexes is the shortening of the Cu–N bond distances in complex **5** as a consequence of the increased oxidation number of Cu (Table 7). The small differences in the conformation of the two complexes (Table 8) can be ascribed more to intraligand steric effects caused by the Li binding in complex **2** than to electronic effects. In complex **5**, the N_4 core is planar with the Cu lying on the N_4 plane, whereas in complex **2**, it shows small but significant tetrahedral distortions, with Cu significantly out of the mean

---

(16) (a) Hathaway, B. J. In *Comprehensive Coordination Chemistry*; Wilkinson, G., Gillard, R. D., McCleverty, J. A., Eds.; Pergamon: Oxford, U.K., 1987; Vol. 5, Chapter 53, p 745 and references therein. (b) Levason, W.; Spicer, M. D. *Coord. Chem. Rev.* **1987**, *76*, 45.

(17) Youngblood, M. P.; Margerum, D. W. *Inorg. Chem.* **1980**, *19*, 3068. Margerum, D. W.; Owens, G. D. In *Metal Ions in Biological Systems*; Sigel, H., Ed.; Dekker: New York, 1981; Vol. 12, p 75. Hamburg, A. W.; Margerum, D. W. *Inorg. Chem.* **1983**, *22*, 3884. Margerum, D. W. *Pure Appl. Chem.* **1983**, *55*, 23. Raycheba, J. M. T.; Margerum, D. W. *Inorg. Chem.* **1983**, *22*, 2139. Diaddario, L. L.; Robinson, W. R.; Margerum, D. W. *Inorg. Chem.* **1983**, *22*, 1021. Fabbrizzi, L.; Perotti, A.; Poggi, A. *Inorg. Chem.* **1983**, *22*, 1411. Owens, G. D.; Phillips, D. A.; Czarnecki, J. J.; Raycheba, J. M. T.; Margerum, D. W. *Inorg. Chem.* **1984**, *23*, 1345. Castellani, C. B.; Fabbrizzi, L.; Licchelli, M.; Perotti, A.; Poggi, A. *J. Chem. Soc., Chem. Commun.* **1984**, 806. Buttafava, A.; Fabbrizzi, L.; Perotti, A.; Poggi, A.; Seghi, B. *Inorg. Chem.* **1984**, *23*, 3917. Fabbrizzi, L.; Forlini, F.; Perotti, A.; Seghi, B. *Inorg. Chem.* **1984**, *23*, 807. Anson, F. C.; Collins, T. J.; Richmond, T. G.; Santarsiero, D.; Toth, J. E.; Treco, B. G. R. T. *J. Am. Chem. Soc.* **1987**, *109*, 2974.

Table 8. Comparison of Structural Parameters for Complexes **2**, **3**, **4**, and **5** (M = Ni for Complex **3**, M = Cu for Complexes **2**, **4**, and **5**)

	2	**3**	**4**	**5**
dist of atoms from N_4 core (Å)	N1, −0.034(3) N2, 0.034(3) N1′, −0.034(3) N2′, 0.034(3) M, −0.057(1)	N1, −0.011(5) N2, 0.011(5) N3, −0.011(5) N4, 0.011(5) M, 0.060(1)	N1, −0.004(5) N2, 0.004(5) N3, −0.007(6) N4, 0.005(5) M, −0.091(1)	N1, −0.010(5) N2, 0.015(6) N1′, −0.010(5) N2′, 0.015(6) M, 0.006(1)
dist of M from N1,C1⋯C4 ring (A) (Å)	−0.446(1)	0.137(1)	0.288(1)	−0.147(1)
dist of M from N2,C6⋯C9 ring (B) (Å)	0.120(1)	−0.010(1)	−0.070(1)	−0.061(1)
dist of M from N3,C11⋯C14 ring (C)[a] (Å)	0.446(1)	−0.669(1)	0.887(1)	0.146(2)
dist of M from N4,C16⋯C19 ring (D)[a] (Å)	−0.120(1)	0.638(1)	0.826(1)	0.061(1)
dihedral angles between the N_4 core and the A, B, C, and D pyrrole rings (deg)	(A) 146.3(1) (B) 149.8(1) (C)[a] 146.3(1) (D)[a] 149.8(1)	156.2(2) 156.6(2) 149.9(2) 152.1(2)	156.4(2) 159.1(2) 146.3(2) 147.5(2)	146.5(1) 147.0(1) 146.5(1) 147.0(1)

[a] For complexes **2** and **5**, the C and D rings are the symmetry-related ones.

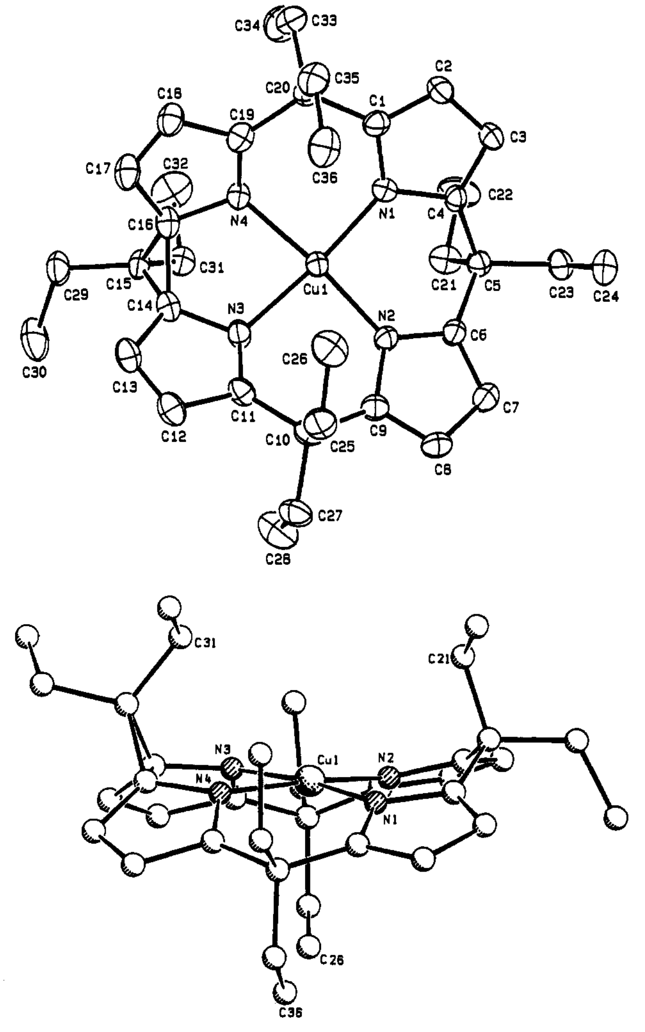

Figure 3. (top) ORTEP view of complex **4** (30% probability ellipsoids). (bottom) A perspective view (SCHAKAL) of complex **4**.

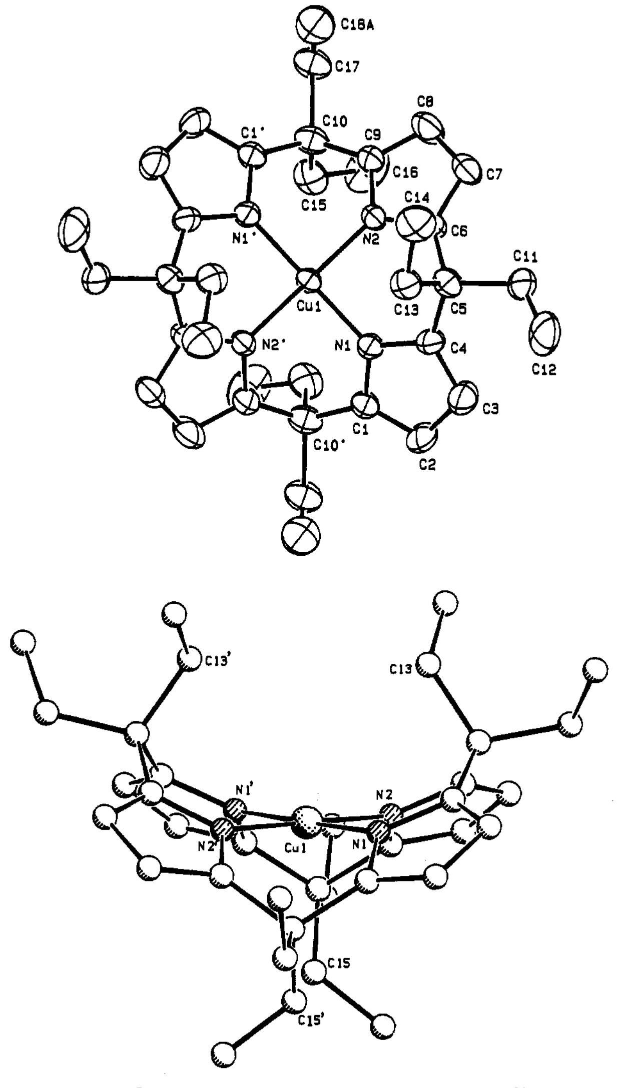

Figure 4. (top) ORTEP view of the anion for complex **5** (30% probability ellipsoids). Primes denote a transformation of *y*, *x*, -*z*. (bottom) A perspective view (SCHAKAL) of complex **5**.

plane by 0.057(1) Å. In addition, the copper atom is out of the plane of the A pyrrole ring by 0.446(1) Å. This distortion is the largest one observed in **2** and **5**. The effect of the lithium binding is also reflected in the asymmetry observed in the Cu–N bond distances (Table 7), which show a small but significant difference. Bond distances and angles within the macrocycle ligand are very similar in complexes **2** and **5** and are in agreement with a π delocalization of the four pyrrole rings. In both complexes four hydrogens atoms from four methylene groups (C11 and C15 for **2**, C13 and C15 for **5**) provide a flattened tetrahedral cage for the copper atom, bisected by the coordination plane. The Cu⋯H distances range from 2.56 to 2.71 Å for **2** and from 2.62 to 2.70 Å for **5**. The same observation has been commented in the case of complex **3** and related references reported.[14,15]

Complex **4** (Figure 3 (top and bottom)) crystallizes with C_6D_6 solvent molecules in a complex:solvent molar ratio of 1:1. The formation of the cyclopropane unit causes some differences in the structural parameters compared with those of complexes **2** and **5** (Tables 8 and 9). In particular, the following can be observed: (i) a significant lengthening of the copper nitrogen (Cu–N3 and Cu–N4) bond distances on forming the cyclopropane unit (Tables 6 and 7); (ii) a larger deviation of the metal from

Table 9. Structural Parameters Related to the Formation of Cyclopropane Unit in Complexes **2**, **3**, **4**, and **5**[a]

	2	**5**
C4···C6 (Å)	2.477(7)	2.400(14)
C9···C1′ (Å)	2.536(5)	2.452(12)
C4–C5–C6 (deg)	108.8(3)	106.0(8)
C9–C10–C1′ (deg)	112.8(3)	108.6(7)

	3	**4**
C1···C19 (Å)	2.541(7)	2.859(9)
C4···C6 (Å)	2.469(9)	2.531(9)
C9···C11 (Å)	2.507(8)	2.559(9)
C14···C16 (Å)	1.567(8)	1.578(9)
C4–C5–C6 (deg)	109.6(5)	111.9(5)
C9–C10–C11 (deg)	113.2(5)	114.6(5)
C14–C15–C16 (deg)	61.9(3)	63.1(4)
C1–C20–C19 (deg)	114.4(5)	116.6(5)

[a] ′ = $-x, y, {}^1/_2 - z$ for **2**. ′ = $y, x, -z$ for **4**.

the N_4 planar core (within the experimental error); (iii) larger displacements of the metal from the C and D pyrrole rings; (iv) a different orientation of the pyrrole rings around the N_4 core, the corresponding dihedral angles involving A and B being significantly larger than those involving C and D, which remain close to the values observed in complexes **2** and **5** (Table 8). These differences can be related to the loss of aromaticity of the C and D rings caused by the formation of the cyclopropane unit. As we observed in complex **3** the bond distances within the C and D rings are consistent with a double bond localization on the N3–C11, N4–C19, C12–C13, and C17–C18 bonds and with the single bond character of N3–C14, N4–C16, and C–C bonds adjacent to the macrocycle (C11–C12, C13–C14, C16–C17, and C18–C19). The A and B rings maintain their bond delocalization as indicated by the related structural parameters. The conformation of **4** is different from those of **2** and **5** in terms of the orientation of the ethyl groups. Two methylene groups (C21 and C31) and two methyl groups (C26 and C36) are arranged on opposite sides around the N_4 core. The H atoms provided by the methylene groups approach more closely the metal on the same side (Cu···H211, 2.73 Å; Cu···H311, 2.72 Å), the other Cu···H contacts being longer than 2.98 Å. This is in agreement with the Cu···C separations which are as follows: Cu···C21, 3.516(7) Å; Cu···C31, 3.408(6) Å; Cu···C26, 3.582(6) Å; Cu···C36, 4.074(6) Å. This finding is similar to, but not the same as, that observed in complex **3**, where only one H atom approaches the Ni atom. The formation of the cyclopropane brings the α-pyrrolic carbons from a distance of *ca.* 2.50 Å in complexes **2** and **5** to a bonding distance of 1.578(9) Å in **4**. This is accompanied by a narrowing of the C14–C15–C16 angle to 63.1(4)° (Table 9).

The configurations at the C14 and C16 asymmetric carbon atoms are *R* and *S*, respectively. Since the space group is acentric, this is the only diastereoisomer present in the structure, the absolute configuration having been unambiguously established by X-ray analysis (see the Experimental Section). As it can be seen from Figures 2 (top) and 3 (top), the configuration of complex **4** is the mirror image of that of complex **3**, so in the solid state, we have the *S*,*R* diastereoisomer for complex **3** and the *R*,*S* diasteroisomer for complex **4**. This may be due to a solid-state self-resolution,[18] or it might just have been coincidence that the different enantiomorphic crystals were selected for the X-ray analysis. We should mention that we carried out the X-ray analysis on **4** after it was recrystallized from THF. This species contains a THF molecule of crystallization and shows the same configuration as **3**, that is, the enantiomer of **4** crystallized from C_6H_6.

Conclusions

We are able to show that the oxidation of the prophyrinogen skeleton, when each *meso*-position is occupied by two alkyl groups, leads to a novel oxidized form of porphyrinogen unlike the porphyrin skeleton. Such an oxidation proceeds with the formation of a cyclopropane unit, which functions as a two-electron shuttle, since its cleavage is easily performed by two-electron reduction. In the case of copper we proved that the formation and cleavage of the cyclopropane unit involves two monoelectronic redox steps, and this led to the isolation of the *meso*-octaethylporphyrinogen–copper(III) complex and to the discovery of an intramolecular metal–ligand redox relationship. An intermolecular electron transfer between metal–porphyrinogen units has been observed in the solvent-dependent disproportionation of **5** occurring in benzene and in the reaction between **2** and **4** leading to **5** in coordinating solvents such as THF.

Experimental Section

General Procedure. All reactions were carried out under a purified nitrogen atmosphere. Solvents were dried and distilled, by standard methods, before use. The syntheses of $[Et_8N_4Li_4(THF)_4]$[8a] and $[Et_8N_4CuLi_2(THF)_4]$[7b] were carried out as reported in previous papers. Infrared, UV–vis, and ^1H NMR spectra were recorded with a Perkin-Elmer 1600 FT-IR spectrophotometer, HP 8452A Diode Array spectrophotometer, and 200-AC Bruker instrument, respectively. The experimental procedure we often used is the extraction of the solid products with the mother liquor following the workup reported in ref 19.

Preparation of 1. Solid $NiCl_2 \cdot THF$ (1.30 g, 6.50 mmol) was added to a THF (120 mL) solution of $[Et_8N_4Li_4(THF)_4]$ (5.60 g, 6.50 mmol), and the resultant suspension was stirred overnight. The resulting red solution was evaporated to dryness and the solid residue extracted with Et_2O. Complex **1** was obtained as a yellow crystalline solid (75%). Anal. Calcd for $C_{52}H_{80}Li_2N_4NiO_4$: C, 69.57; H, 8.98; N, 6.24. Found: C, 69.11; H, 8.94; N, 6.71. ^1H NMR (C_6D_6): δ 6.17 (s, 8 H, C_4H_2N), 3.25 (m, 16 H, THF), 3.25 (q, 8 H, CH_2), 2.26 (q, 8 H, CH_2), 1.25 (t, 12 H, CH_3), 1.21 (m, 16 H, THF), 1.01 (t, 12 H, CH_3). UV-vis (THF): λ 254 nm (ϵ 15 000 cm^{-1} M^{-1}), 298 (18 000), 430 (2 400).

Preparation of 3 Using *p*-Benzoquinone. A Et_2O (100 mL) solution of *p*-benzoquinone (3.80 g, 35.0 mmol) was added dropwise to a Et_2O solution of **1** (8.0 g, 8.80 mmol). A blue solid, a red solid, and a deep-red solution were rapidly formed. The suspension was stirred at room temperature for 1 day, after which an extraction of the solid mixture with the mother liquor allowed removal of the blue solid (lithium quinhydrone). The resulting solution was evaporated to dryness and the solid residue washed with *n*-hexane (2 × 50 mL) to give the red crystalline solid of **3** (56%). Anal. Calcd for $C_{36}H_{48}N_4Ni$: C, 72.60; H, 8.10; N, 9.40. Found: C, 72.64; H, 8.25; N, 9.59. The solid recrystallized from THF/*n*-hexane gave crystals suitable for X-ray analysis, containing a THF molecule of crystallization. Anal. Calcd for $C_{40}H_{56}N_4NiO$: C, 71.95; H, 8.45; N, 8.38. Found: C, 71.90; H, 8.08; N, 8.28. The ^1H NMR spectrum was run on the crystals used for the X-ray analysis. ^1H NMR (C_6D_6, room temperature): δ 6.61 (d, 2 H, J = 3.3 Hz), 6.59 (d, 2 H, J = 5.6 Hz), 6.38 (d, 2 H, J = 3.3 Hz), 6.11 (d, 2 H, J = 5.6 Hz), 3.57 (q, 2 H), 3.57 (m, 4 H, THF), 2.81 (q, 2 H), 2.56 (q, 2 H), 2.29 (m, 2 H), 1.81 (q, 4 H), 1.61 (m, 2 H), 1.43 (t, 3 H), 1.41 (t, 3 H), 1.41 (m, 4 H, THF), 1.17 (q, 2 H), 1.06 (t, 6 H), 0.73 (t, 6 H), 0.71 (t, 3 H), 0.43 (t, 3 H). UV–vis (THF): λ 264 nm (ϵ_{Ni} 31 600 cm^{-1} M^{-1}), 350 (15 630), 474 (3 040).

Preparation of 3 Using Iodine. Iodine (0.30 g, 1.20 mmol) was added to a Et_2O (70 mL) solution of **1** (1.10 g, 1.20 mmol), and the resulting suspension was stirred for 1 day. An extraction with the mother liquor removed the insoluble LiI. On reduction of the solution of 30 mL, **3** precipitated as a red crystalline solid. The IR spectrum is superimposable with that from *p*-benzoquinone oxidation. The solid contained some LiI, as revealed by the microanalysis. Anal. Calcd for $C_{36}H_{48}N_4Ni(LiI)_{0.25}$: C, 68.75; H, 7.69; N, 8.91. Found: C, 68.75; H, 8.01; N, 9.06.

Preparation of 4 Using *p*-Benzoquinone. A Et_2O (50 mL) solution of *p*-benzoquinone (0.19 g, 1.80 mmol) was added dropwise to a Et_2O (70 mL) solution of **2** (0.80 g, 0.89 mmol). A blue solid and a red solid rapidly formed. The deep-red suspension was stirred overnight, then extracted with the mother liquor in order to remove the insoluble blue

---

[18] (a) Jacques, J.; Collet, A.; Wilen, S. H. *Enantiomers, Racemates and Resolutions*; Wiley: New York, 1981; pp 14–18. (b) Caswell, L.; Garcia-Garibay, M. A.; Scheffer, J. R.; Trotter, J. *J. Chem. Educ.* **1993**, *70*, 785.

[19] Floriani, C.; Mange, V. In *Inorganic Syntheses*; Angelici, R. J., Ed.; Wiley: New York, 1990; Vol. 28, pp 263–267.

solid (lithium quinhydrone). The solution was reduced to 30 mL, then allowed to stand to give red-violet crystals of **4** (60%). Anal. Calcd for $C_{36}H_{48}CuN_4$: C, 72.02; H, 8.06; N, 9.33. Found: C, 72.34; H, 8.09; N, 8.99. μ_{eff} = 1.82 BM at 293 K. UV–vis (THF): λ 256 nm (ε 25 000 cm^{-1} M^{-1}), 296 (32 800), 518 (10 000).

Preparation of 5 from the Oxidation of 2 with $CuCl_2$. $CuCl_2(THF)_{0.5}$ (0.16 g, 0.90 mmol) was added to a THF (70 mL) red solution of **2** (0.84 g, 0.90 mmol). A blue solution rapidly formed. The solvent was removed under reduced pressure, and the resultant solid was extracted with toluene (100 mL). The insoluble salts were filtered off to yield a red solution. The toluene solution was evaporated to dryness and the solid dissolved in the minimum amount of THF to obtain a blue solution. The addition of *n*-hexane to the THF solution gave blue crystals of **5** (85%). Anal. Calcd for $C_{52}H_{80}CuN_4LiO_4$: C, 69.73; H, 9.00; N, 6.25. Found: C, 69.00; H, 8.75; N, 6.02. ^1H NMR (C_4H_8O): δ 5.71 (s, 8 H, C_4H_2N), 2.15 (q, 16 H, CH_2), 1.85 (m, THF), 1.12 (t, 12 H, CH_3), 0.65 (t, 12 H, CH_3). ^1H NMR ($(CD_3)_2CO$): δ 5.86 (s, 8 H, C_4H_2N), 3.80 (m, 16 H, THF), 2.22 (q, 16 H, CH_2), 1.31 (t, 12 H, CH_3), 0.74 (t, 12 H, CH_3). UV–vis (THF): λ 236 nm (ε 28 530 cm^{-1} M^{-1}), 268 (30 060), 596 (2 780).

Preparation of 4 from the Oxidation of 5 with $CuCl_2$. $CuCl_2(THF)_{0.5}$ (0.16 g, 0.90 mmol) was added to a blue THF (70 mL) solution of **5** (0.86 g, 0.96 mmol). The deep-red violet suspension was stirred for 1 day, then evaporated to dryness. The solid residue was dissolved in toluene (100 mL), and the insoluble salts were removed by filtration. The toluene was removed under reduced pressure and the residue dissolved in THF (20 mL). On addition of *n*-hexane (60 mL) and cooling of the solution at –4 °C, solid **4** was formed (81%). The solid contained LiCl. The IR spectrum is superimposable with that of **4** obtained from the oxidation with *p*-benzoquinone. Anal. Calcd for $C_{36}H_{48}ClCuN_4Li$: C, 67.27; H, 7.53; N, 8.72. Found: C, 66.80; H, 7.58; N, 8.54.

Preparation of 5 from Equimolar Amounts of 2 and 4. A solid equimolar mixture of **2** (0.38 g, 0.42 mmol) and **4** (0.25 g, 0.42 mmol) was treated with THF (50 mL) to give a blue solution from which, by addition of *n*-heptane (20 mL), crystals of **5** were obtained (93%).

Disproportionation of 5 in Benzene. Complex **5** (0.30 g, 0.34 mmol) was dissolved in benzene (15 mL), and the resulting red solution was allowed to stand at 0 °C for 2 days. A mixture of well-formed red-violet (**4**) and orange (**2**) crystals was formed. Suitable crystals were selected for X-ray structure analysis on **4**.

Preparation of 6. 12-Crown-4 (0.20 g, 1.20 mmol) was added to a THF (60 mL) solution of **5** (1.10 g, 1.20 mmol). The solution was stirred for 2 h, then *n*-hexane (30 mL) was added to give a violet crystalline solid (68%). Complex **6** is only poorly soluble in benzene but is more soluble in CH_2Cl_2. Anal. Calcd for $C_{44}H_{64}CuN_4LiO_4$: C, 67.45; H, 8.23; N, 7.15. Found: C, 67.04; H, 8.40; N, 7.30. ^1H NMR (CD_2Cl_2): δ 5.76 (s, 8 H, C_4H_2N), 3.62 (bs, 12-crown-4), 2.08 (q, 16 H, CH_2), 1.14 (t, 12 H, CH_3), 0.54 (t, 12 H, CH_3).

Reduction of 4 to 5 with Lithium Metal. A violet solution (70 mL) of **4** (0.80 g, 1.30 mmol) was reduced with lithium sand (0.011 g, 1.50 mmol) under argon. The suspension was stirred for 2 h to give a blue solution. The solution was reduced under vacuum to 20 mL, and *n*-hexane was added to the reduced solution until **5** started to crystallize (73%). Complex **5** was identified by its NMR spectrum and microanalysis.

Reduction of 4 to 2 with Excess Lithium Metal. An excess of lithium sand (0.021 g, 3.0 mmol) was added to a THF (70 mL) solution of **4** (0.45 g, 0.75 mmol). A blue solution of **5** was rapidly obtained (*ca.* 30 min). Continuous stirring for an additional 1 day gave an orange solution. Excess lithium was filtered off, the solvent was partially evaporated, and **2** was crystallized upon addition of *n*-heptane (20 mL). Complex **2** was identified by microanalysis and its IR spectrum.

Reductive Demetalation of 4 with H_2S. A solution of **4** (0.53 g, 0.88 mmol) was saturated with H_2S. In ca. 10 min a brown suspension was obtained. The suspension was stirred for 2 h, then the mixture was evaporated to dryness. The solid was extracted with *n*-hexane (50 mL), and the brown solid was removed by filtration. On evaporation, the hexane solution gave $Et_8N_4H_4$ (84%).

Reduction of 3 to 1 Using Lithium Metal. A THF (70 mL) solution of **3** (0.44 g, 0.73 mmol) was treated with excess lithium metal (0.020 g, 2.80 mmol) and biphenyl (0.005 g). The suspension gave a yellow-green solution on stirring for 1 day. Excess lithium was removed by filtration, and **1** was recovered upon partial evaporation of the solvent and addition of *n*-hexane (50 mL). In the absence of biphenyl the reduction did not occur.

X-ray Crystallography. The crystals of compounds **2**, **3**, **4** and **5** were mounted in glass capillarities and sealed under nitrogen. The reduced cells were obtained with use of TRACER.[20] Crystal data and details associated with structure refinement are given in Table 1. Data were collected at room temperature (295 K) on a single-crystal diffractometer. For intensities and background, individual reflection profiles were analyzed.[21] The structure amplitudes were obtained after the usual Lorentz and polarization corrections and the absolute scale was established by the Wilson method.[22] Data were corrected for absorption using the program ABSORB[23] for complex **2** and a semiempirical method[24] for complexes **4** and **5**. No absorption correction was carried out for complex **3**. The function minimized during the full-matrix least-squares refinement was $\sum w|\Delta F|^2$. A weighting scheme $\{w = k/[\sigma^2(F_o) + g|F_o|^2]\}$ based on counting statistics was applied for complexes **2** and **3**.[25] For complexes **4** and **5**, unit weights were applied since these gave the most satisfactory analysis of variance and the best agreement factors. Anomalous scattering corrections were included in all structure factor calculations.[26b] Scattering factors for neutral atoms were taken from ref 26a for non-hydrogen atoms and from ref 27 for H. Among the low-angle reflections no correction for secondary extinction was deemed necessary. All calculations were carried out on an IBM-AT personal computer equipped with an INMOS T800 Transputer and an ENCORE 91 computer using SHELX-76.[25] Solution and refinement were based on the observed reflections. The structures were solved by the heavy-atom method by starting from a three-dimensional Patterson map.

Complex 2. Refinement was done first isotropically, then anisotropically, for all non-H atoms. All the hydrogen atoms were located from difference Fourier maps and introduced in the final refinement as fixed atom contributions (isotropic *U*'s fixed at 0.10 Å^2). The final difference map showed no unusual features, with no significant peaks above the general background.

Complex 3. Refinement was done first isotropically, then anisotropically, for all non-H atoms, except for the C24 methyl carbon atom and the C42–C45 atoms of the THF molecule of crystallization which were found to be affected by disorder. The disorder was solved by splitting the involved atoms over two positions (A and B) which were isotropically refined with the site occupation factors given in Table 3 by constraining the C–C bond distances within the THF molecule to be 1.54 Å (no possibility to distinguish between oxygen and carbon). All the hydrogen atoms, but those associated to the disordered atoms and to the methylene carbon C23, which were ignored, were located from difference Fourier maps and introduced in the final refinement as fixed atom contributions (isotropic *U*'s fixed at 0.12 Å^2). The final difference map showed no unusual features, with no peaks above the general background. Since the space group is acentric, the crystal chirality was tested by inverting all the coordinates ($x, y, z \backslash -x, -y, -z$) and refining to convergence once again. The resulting *R* values indicated the previous choice should be considered the correct one (Table 1). The coordinates quoted in Table 3 refer to the original choice.

Complex 4. Refinement was done first isotropically, then anisotropically, for all the non-H atoms. All the hydrogen atoms were located from difference Fourier maps and introduced in the final refinement as fixed atom contributions (isotropic *U*'s fixed at 0.08 Å^2). During the refinement the phenyl ring of the deuterated benzene molecule of crystallization was constrained to be a regular hexagon (C–C = 1.395 Å). The final difference map showed no unusual features, with no peaks having significant meaning above the general background. The crystal chirality was tested as above (complex **2**). The resulting *R* values indicated the "inverted structure" should be considered the correct one (Table 1). The coordinates quoted in Table 4 refer to the "inverted structure".

Complex 5. Refinement was done first isotropically, then anisotropically, for all non-H atoms, except for the C18 methyl carbon and the

---

(20) Lawton, S. L.; Jacobson, R. A. *TRACER (a cell reduction program)*; Ames Laboratory, Iowa State University of Science and Technology: Ames, IA, 1965.

(21) Lehmann, M. S.; Larsen, F. K. *Acta Crystallogr., Sect. A: Cryst. Phys., Diffr., Theor. Gen. Crystallogr.* **1974**, *A30*, 580–584.

(22) Wilson, A. J. C. *Nature* **1942**, *150*, 151.

(23) Ugozzoli, F. ABSORB, a Program for F_o Absorption Correction. *Comput. Chem.* **1987**, *11*, 109.

(24) North, A. C. T.; Phillips, D. C.; Mathews, F. S. *Acta Crystallogr., Sect. A: Cryst. Phys., Diffr., Theor. Gen. Crystallogr.* **1968**, *A24*, 351.

(25) Sheldrick, G. *SHELX-76: System of Crystallographic Computer Programs*; University of Cambridge: Cambridge, England, 1976.

(26) (a) *International Tables for X-ray Crystallography*; Kynoch Press: Birmingham, England, 1974; Vol. IV, p 99. (b) *Ibid.* p 149.

(27) Stewart, R. F.; Davidson, E. R.; Simpson, W. T. *J. Chem. Phys.* **1965**, *42*, 3175.

C21, C23, C24, C25, C26, and C28 carbons of the $[Li(THF)_4]^+$ cation which were found to be affected by disorder. The disorder was solved by splitting the involved atoms over two positions (A and B) isotropically refined with the site occupation factors given in Table 5. All the hydrogen atoms, but those associated to disorder, which were ignored, were put in geometrically calculated positions and introduced in the final refinement as fixed atom contributions (isotropic *U*'s fixed at 0.10 Å^2). The final difference map showed no unusual features with no peaks above the general background.

Final atomic coordinates are listed in Tables 2–5 for non-H atoms and in supplementary Tables SII–SV for hydrogens. Thermal parameters are given in Tables SVI–SIX, bond distances and angles in Tables SX–SXIII.[28]

Acknowledgment. We would like to thank the Fonds National Suisse de la Recherche Scientifique (Grant No. 20–33420–92) for financial support.

Supplementary Material Available: Tables giving crystal data and details of the structure determination, hydrogen atom coordinates, anisotropic and isotropic thermal parameters, bond lengths, and bond angles and a figure showing an ORTEP view of the cation in **5**. (17 pages); listings of structure factors (39 pages). This material is contained in many libraries on microfiche, immediately follows this article in the microfilm version of the journal, and can be ordered from the ACS; see any current masthead page for ordering information.

---

[28] See paragraph at the end regarding supplementary material.